

Small Punch Creep Life Prediction from Steady-State Deflection Rate in High-Chromium Ferritic Heat-Resistant Steels



NAVEENA and SHIN-ICHI KOMAZAKI

The small punch (SP) creep deformation and rupture behavior of different high-chromium ferritic heat-resistant steels were studied at various temperatures in the range from 923 K to 1073 K (650 °C to 800 °C) and loads in the range from 65 to 400 N. The creep deflection rate, after an initial abrupt decrease, showed no significant variation during most of the creep time and exhibited a steady-state creep stage. The time to steady-state creep stage accounted for less than 30 pct of the creep rupture life. A close relationship was found to exist between steady-state deflection rate and time to rupture, resembling Monkman–Grant relation. This relationship was independent of the type of steels studied, resulting in a single master curve. This relationship was used for predicting SP creep rupture life. The predicted rupture life was within an accuracy factor of 1.2. The study revealed that the creep rupture life can be reasonably well predicted by evaluating steady-state deflection rate, without waiting for the fracture of specimen to occur. This approach of prediction using steady-state deflection rate was found to be more advantageous than that using minimum deflection rate as the latter appeared relatively close to the onset of acceleration creep.

<https://doi.org/10.1007/s11661-019-05121-3>

© The Minerals, Metals & Materials Society and ASM International 2019

I. INTRODUCTION

CREEP rupture life in conventional uniaxial creep tests can be predicted using minimum creep rate from the Monkman–Grant model,^[1] which defines relationship between the minimum creep rate and time to rupture. The small punch (SP) creep test which utilizes small specimens can be employed as an effective tool for evaluating creep rupture properties of materials.^[2–8] The test method can determine creep properties with a high accuracy because of a kind of destructive test. Since the test needs miniaturized specimen (diameter: 3 to 10 mm and thickness: 0.25 to 0.5 mm),^[9] it is advantageous over conventional full scale creep test. A great amount of effort has been made by a number of researchers to deepen the understanding of both, the SP creep test results and its correlation to conventional uniaxial creep test results, and it is still evolving. The applicability of Monkman–Grant relationship in SP creep test has been

investigated by a number of authors.^[10–14] It was found that the minimum deflection rate can be well correlated to the time to rupture. In SP creep test, the minimum deflection rate appears in the latter half of creep life, just before the onset of acceleration creep, unlike in uniaxial creep tests. As a result, to determine minimum deflection rate, one has to carry out the SP creep test until almost the rupture of specimen. In this regard, instead of minimum deflection rate, if the steady-state deflection rate that would appear prior to minimum deflection rate is available and can be used for predicting creep rupture life then it is more advantageous. This would permit one to forego the necessity of running the creep test until rupture of the specimen.

In SP creep test, the relationship between steady-state deflection rate and time to rupture has not been analyzed so far. Therefore, the present study was undertaken to investigate steady-state creep deformation as well as rupture behavior and their interrelationship in high-chromium ferritic heat-resistant steels and to analyze the possibility of predicting creep rupture life using steady-state deflection rate. We investigated this in different high-chromium ferritic heat-resistant steels which vary by its chemical compositions, heat-treatment conditions and microstructures with a view to examine their influence on steady-state deflection rate–time to rupture correlation and prediction of creep rupture life from this correlation.

NAVEENA is with the Division of Mechanical Engineering, Graduate School of Science and Engineering, Kagoshima University, Kagoshima 890-0065, Japan. Contact e-mail: naveena@mech.kagoshima-u.ac.jp
SHIN-ICHI KOMAZAKI is with the Research Field in Engineering, Science and Engineering Area, Research and Education Assembly, Kagoshima University, Kagoshima 890-0065, Japan.

Manuscript submitted August 3, 2017.

Article published online January 23, 2019

II. EXPERIMENTAL PROCEDURE

The high-chromium ferritic heat-resistant steels considered for the present investigation include conventional Gr.91 steel, PN1 steel, and different heats of high-nitrogen (HN) ferritic steels. The chemical compositions (in wt pct) and heat-treatment conditions of each steel are given in Table I. The Gr.91, PN1, and HN1 to 9L were normalized and tempered steels. They exhibited tempered martensite microstructure. The typical examples of these tempered martensite microstructures have been reported previously.^[15,16] The HN10 was a normalized steel and consisted of a fully ferrite structure as discussed in the previous study.^[16] Since these steels (especially high-nitrogen grade steels) are still under development in this research program, further details of their microstructures are not reported in this study. It can be noted that HN9 and HN9L had the same chemical compositions but were subjected to different heat-treatment conditions with an original intention of examining the influence of heat treatment on creep rupture strength, as was discussed in the previous study.^[16] The SP creep tests were performed in the temperature range from 923 K to 1073 K (650 °C to 800 °C), under constant loads in the range from 65 to 400 N, using disk-type specimens of dimension $\varnothing 8 \times 0.5$ mm. The thickness of specimen was carefully adjusted to 0.5 ± 0.005 mm by grinding and polishing both sides. The final surface finish was done using $0.3 \mu\text{m}$ Al_2O_3 . The SP creep machine and the test-rig used in this study are shown in Figure 1. The test specimen was clamped between the upper and lower dies, as schematically shown in Figure 1. A constant load was applied on the specimen surface through a Si_3N_4 ball ($\varnothing 2.38$ mm) when the test temperature was stabilized. The displacement of the ball was continuously measured as central deflection using a linear variable differential transducer (LVDT). All the tests were performed in a high-purity (99.99 pct) argon gas atmosphere in order to protect the specimen, puncher, upper, and lower dies from severe oxidation. The specimen temperature was maintained within ± 1 K (± 1 °C) of the test temperature during the tests.

III. RESULTS AND DISCUSSION

A. SP Creep Deformation and Rupture Behavior

Typical central deflection-time behavior, *i.e.*, the SP creep curves, of Gr.91 and HN steels (HN9, HN9L and HN10), measured at 973 K (700 °C) under 220 N and 300 N, are shown in Figure 2. As generally seen and also discussed in our previous study,^[16] the SP creep curves were only qualitatively similar to those of standard uniaxial creep tests. This is because of the fact that there are differences in terms of the test fixture and methodology, the state of stress, and mode of deformation that occur in the specimens during these creep tests. Since the uniaxial creep curves of these steels are being analyzed and not available at this moment, the comparison of SP and uniaxial creep curves could not be made. However, a recent study by Ganesh Kumar *et al.*^[3] showed a close relationship between the SP and uniaxial transient and tertiary creep behavior in 316LN stainless steel. As generally observed in any SP creep test, these SP creep curves showed a relatively large instantaneous deflection upon loading due to plastic bending deformation of the specimen. This deflection was followed by primary, secondary, and tertiary stages of creep. There was no clear effect of applied load and test temperature on the central deflection at rupture, and all the specimens

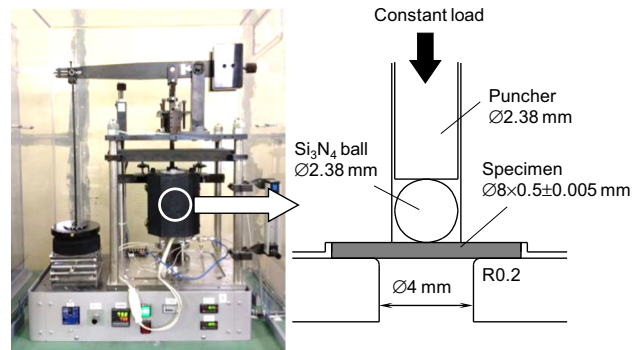


Fig. 1—SP creep machine and test-rig used in this study.

Table I. Chemical Compositions and Heat-Treatment Conditions of the Steels Used

Steels	Chemical Composition (Weight Percent)													
	C	N	Cr	Mo	V	Nb	W	Co	Mn	Ni	Si	Ti	Cu	Fe
Gr.91	0.10	0.04	8.28	0.88	0.20	0.06	—	—	0.44	0.07	0.06	.008	—	bal.
PN1	0.10	0.60	16.0	1.1	0.22	—	—	—	0.16	0.16	—	—	0.15	bal.
HN1	0.021	0.60	9.31	—	2.1	—	—	—	0.09	0.03	0.09	—	—	bal.
HN5	0.014	0.33	9.26	—	1.28	0.02	1.03	2.01	0.07	0.02	0.04	—	—	bal.
HN9/9L	0.010	0.32	9.06	1.04	0.60	0.02	5.97	4.0	0.07	0.01	0.06	—	—	bal.
HN10	0.015	0.34	15.0	1.00	1.30	0.02	6.0	4.0	0.07	0.01	0.06	—	—	bal.

Gr.91: 1323 K (1050 °C) – 60 min (normalizing) + 1053 K (780 °C) – 60 min (tempering).
 PN1: 1373 K (1100 °C) – 30 min (normalizing) + Subzero (~353 K (80 °C)) + 1053 K (780 °C) – 30 min (tempering).
 HN1: 1473 K (1200 °C) – 30 min (normalizing) + 1043 K (770 °C) – 30 min (tempering).
 HN5: 1473 K (1200 °C) – 30 min (normalizing) + 1053 K (780 °C) – 60 min (tempering).
 HN9: 1473 K (1200 °C) – 30 min (normalizing) + 1053 K (780 °C) – 60 min (tempering).
 HN9L: 1473 K (1200 °C) – 30 min (normalizing) + 973 K (700 °C) – 45 h (tempering).
 HN10: 1473 K (1200 °C) – 30 min (normalizing).

ruptured when the central deflection reached approximately 2.5 mm, irrespective of the test conditions.

Figure 3 shows the variation of central deflection rate with creep time corresponding to the SP creep curves shown in Figure 2. The central deflection rate abruptly decreased upon load application. Then, it attained a constant value and showed no significant change for a long duration, almost until final acceleration creep stage. A steady-state creep stage was exhibited. A similar deformation behavior was observed in other steels in this study. The constant deflection rate in the steady-state creep region was considered as the steady-state deflection rate, $\dot{\delta}_s$. Figure 4 shows an example of the influence of applied load on steady-state deflection rate in HN9L, tested at 998 K (725 °C) under 140 N and 300 N. The steady-state deflection rate decreased with the decreasing applied load. The $\dot{\delta}_s$ at 140 N was

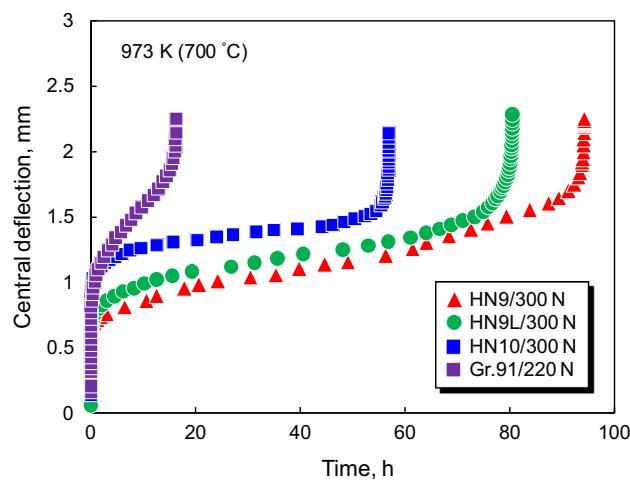


Fig. 2—Typical central deflection-time behavior of the conventional steel (Gr.91) and HN steels (HN9, HN9L, and HN10) at 973 K (700 °C) under different loads.

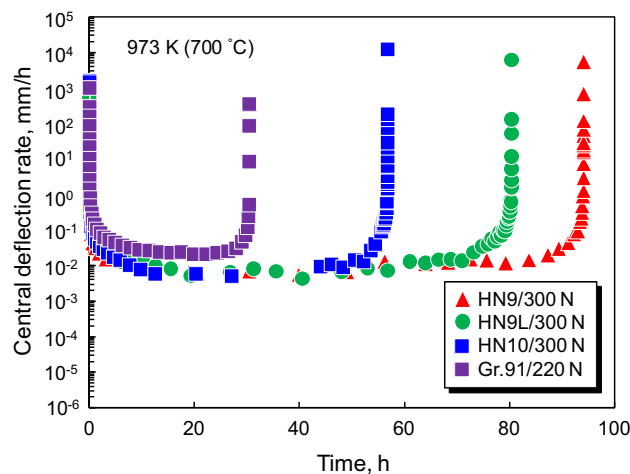


Fig. 3—Typical central deflection rate-time behavior of the conventional steel (Gr.91) and HN steels (HN9, HN9L, and HN10) at 973 K (700 °C) under different loads.

approximately one order magnitude lower than that at 300 N.

The time to onset of steady-state deflection rate was analyzed. Figure 5 shows the plot of time to reach steady-state deflection rate (t_s), in comparison with time to reach minimum deflection rate (t_{\min}), against the time to rupture (t_r). Both t_s and t_{\min} were normalized to t_r . The t_{\min} was obtained as the time corresponding to the minimum value of deflection rate from the central deflection rate-time curve (double-logarithmic scale). To determine t_s , the steady-state deflection rate ($\dot{\delta}_s$) was first determined by a least square method. For this, the region of steady-state was identified in the central deflection rate-time curves (semi-logarithmic scale). The deflection rates in this region were considered to determine $\dot{\delta}_s$ from the least square method. Then, the t_s was obtained as the point of intersection of straight line of steady-state deflection rate with the central deflection rate-time curve. From the result, it was found that the

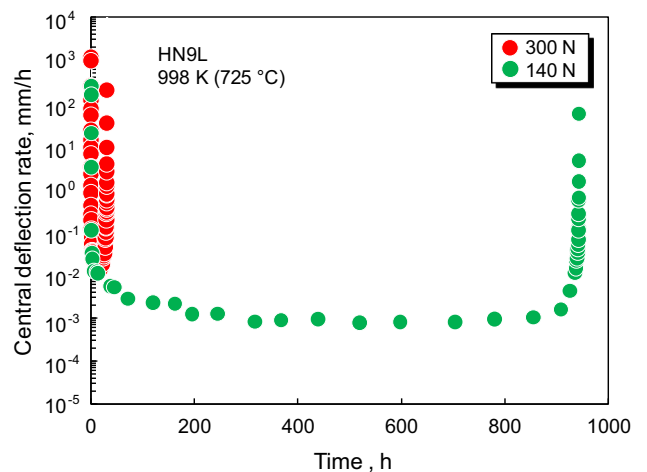


Fig. 4—An example of effect of applied load on central deflection rate-time behavior in HN9L at 998 K (725 °C).

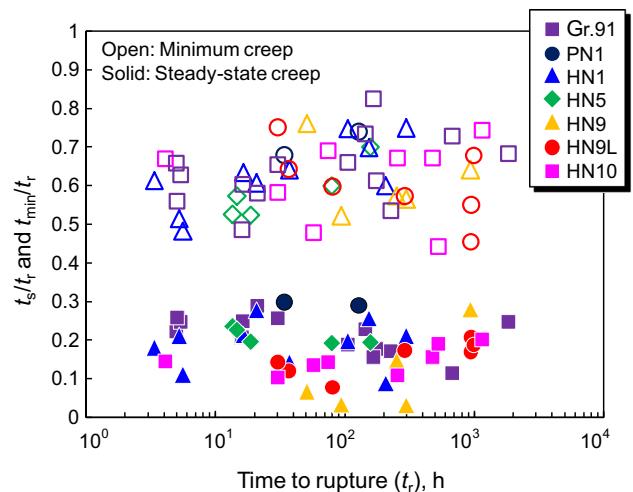


Fig. 5—The plot of ratios t_s/t_r and t_{\min}/t_r as a function of t_r .

time to onset of steady-state creep stage accounted for less than 25 to 30 pct of the creep rupture life. On the other hand, the minimum deflection rate attained in the latter half of the creep rupture life, accounting for 50 to 80 pct of creep rupture life, although some scatter was seen. One can see a relatively large difference between the time to reach steady-state and minimum deflection rate, the former appearing in the much early stage of creep. Since the period of acceleration creep stage is relatively short in SP creep test when compared with that in a conventional uniaxial creep test and the minimum deflection rate appears in the latter half of rupture life in SP creep test, it is not very practical to exploit the minimum deflection rate for predicting rupture life. Therefore, as mentioned previously, if the steady-state deflection rate is available in place of the minimum deflection rate, it is very useful for creep life prediction. To this end, we investigated the relationship between steady-state deflection rate and time to rupture and analyzed the possibility of using this relationship for predicting creep rupture life which is discussed in the preceding sections.

The relationship between the steady-state deflection rate ($\dot{\delta}_s$) and time to rupture (t_r), plotted on a double-logarithmic scale, is shown in Figure 6(a). Here, the $\dot{\delta}_s$ was determined by the least square method, as explained above. The steady-state deflection rate was found to be well correlated with the time to rupture, regardless of the test temperatures and loads, which followed a relationship similar to a Monkman–Grant relation. Furthermore, the results were found to be almost independent of the type of steels studied, yielding a single master curve. To be more specific, this relationship was not dependent on whether the microstructure of steel was tempered martensite or ferrite. It was also observed that the relationship was independent of the heat-treatment conditions of HN9 and HN9L, which essentially did not show any significant difference in their creep rupture strength in the previous study.^[16] Figure 6(b) shows the relationship between minimum deflection rate ($\dot{\delta}_{min}$) and time to rupture (t_r), plotted on a double-logarithmic scale. This relationship was also found to follow a Monkman–Grant type relation, with no significant dependence on the kind of steels studied, the test temperatures and loads. This type of correlation was reported on various materials.^[10–14] The interrelationship between the steady-state deflection rate and minimum deflection rate was examined. Figure 7 shows the double-logarithmic plot of steady-state and minimum deflection rates. A relatively good correlation was found to exist between the two parameters, independent of the steels, test temperatures and loads, although they showed a slight deviation from each other. The reason for this deviation could be the scatter in data points in the central deflection rate–time curves. This scatter could result in small difference in the minimum and steady-state deflection rate values as the former was directly obtained from the central deflection rate–time curves and the latter determined by the least square fit. This was examined by comparing the steady-state deflection rates and minimum deflection rates at

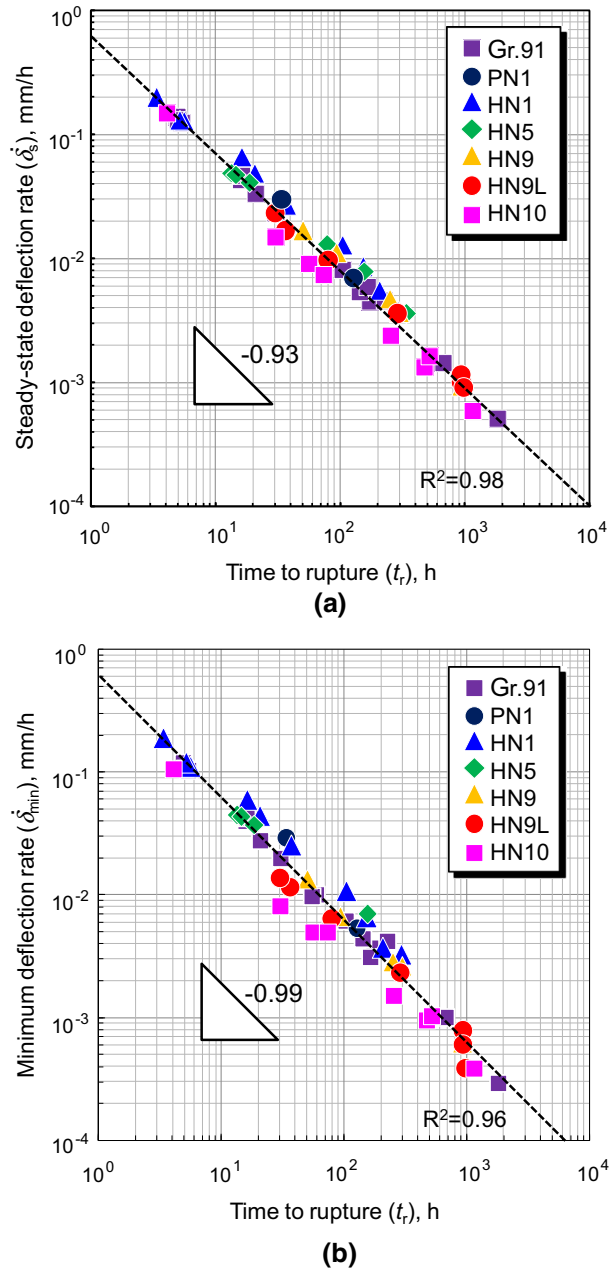


Fig. 6—Relationship between (a) steady-state deflection rate and time to rupture and (b) minimum deflection rate and time to rupture.

different loads and temperatures. Figures 8(a) and (b) shows such comparisons at 923 K and 973 K (650 °C and 700 °C), respectively. Although the steady-state deflection rates and minimum deflection rates were in close agreement in some of the steels at some test conditions, they showed slight differences in some of the steels under other test conditions. However, it is to be noted that despite this deviation the rupture life could be well predicted which can be seen in the following section.

Figure 9 shows the double-logarithmic plot of variation of steady-state and minimum deflection rate with applied load for different steels at 973 K (700 °C). A

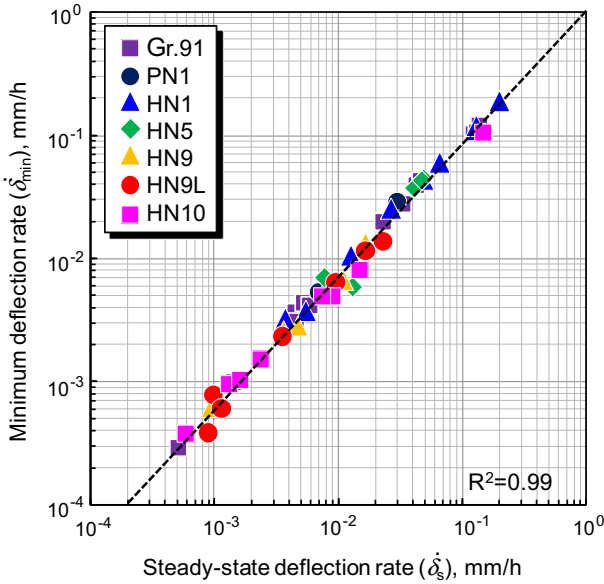


Fig. 7—Relationship between steady-state deflection rate and minimum deflection rate.

power-law relationship was found to be obeyed. The load exponents of the steady-state deflection rates, N_s , and the minimum deflection rates, N_{min} , were compared. Both N_s and N_{min} were found to be comparable in all the steels. The load exponent of Gr.91 steel was higher than those of the HN steels.

B. Creep Rupture Life Prediction from Steady-State Deflection Rate

Determination of t_s and $\dot{\delta}_s$ from a complete creep curve (Figure 3), after the test, is by no means difficult. However, the identification of an accurate t_s and estimation of $\dot{\delta}_s$ in an ongoing SP creep test is not so easy as it is difficult to judge whether the creep deflection rate has reached a steady-state. Therefore, in this study, the effect of creep testing time on the accuracy of life prediction was simulated. The results of such simulations are shown in Figure 10 as examples on HN9L and HN10. The results presented in Figure 10(a) correspond to the short-time creep tests with rupture life of approximately 200 hours, at 973 K (700 °C)/220 N. The results in Figure 10(b), on the other hand, represent the long-time creep tests with rupture life of approximately 1000 hours, at 998 (725 °C)/140 N. The accuracy, *i.e.*, the ratio of predicted rupture life to the observed rupture life, t'_r/t_r , was plotted as a function of test time ratio, t/t_s . Also plotted in the graphs were the estimated steady-state deflection rates, $\dot{\delta}'_s$, against t/t_s . The $\dot{\delta}'_s$ were estimated using the data obtained after certain testing time, t . The method of estimation of $\dot{\delta}'_s$ is explained later in this section. The rupture life for each estimated $\dot{\delta}'_s$ was predicted using the steady-state deflection rate–time to rupture relationship (Figure 6(a)). The $\dot{\delta}'_s$ gradually

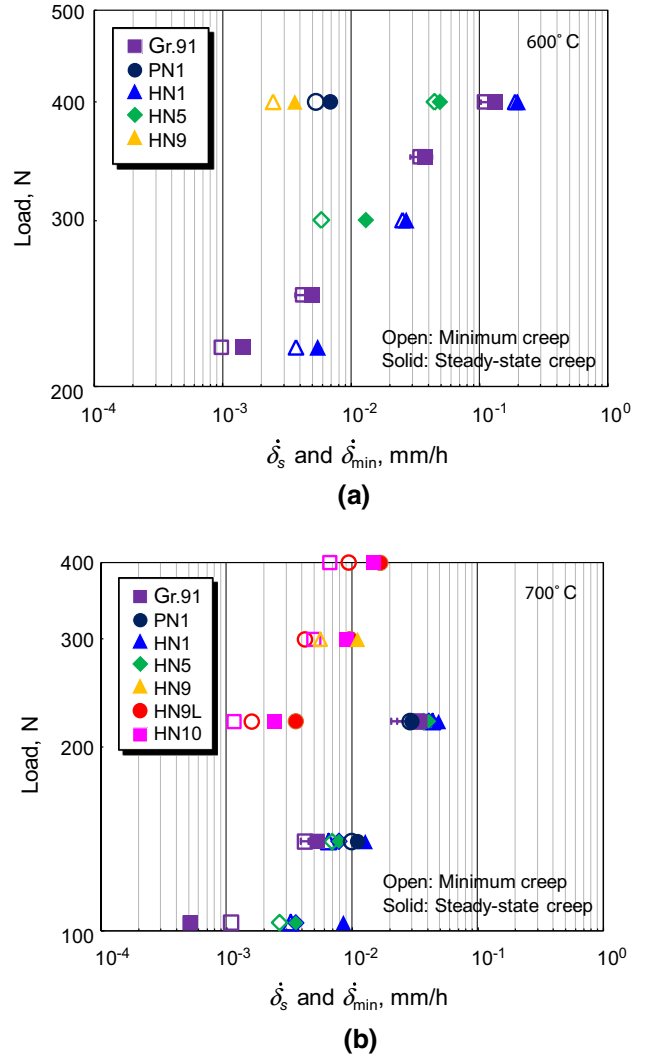


Fig. 8—Comparison of steady-state deflection rates and minimum deflection rates at different SP loads at (a) 923 K (650 °C) and (b) 973 K (700 °C).

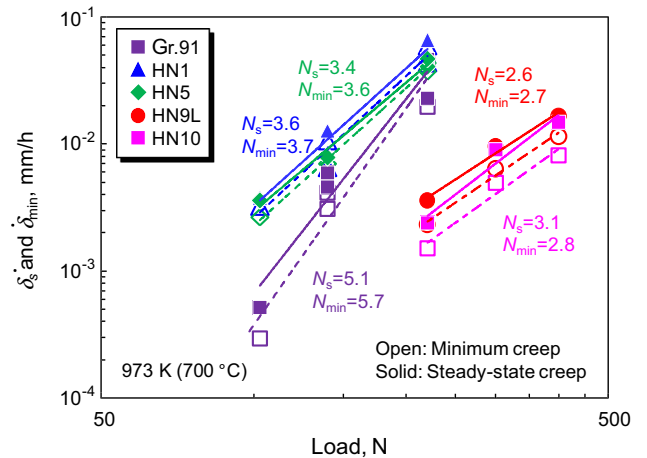
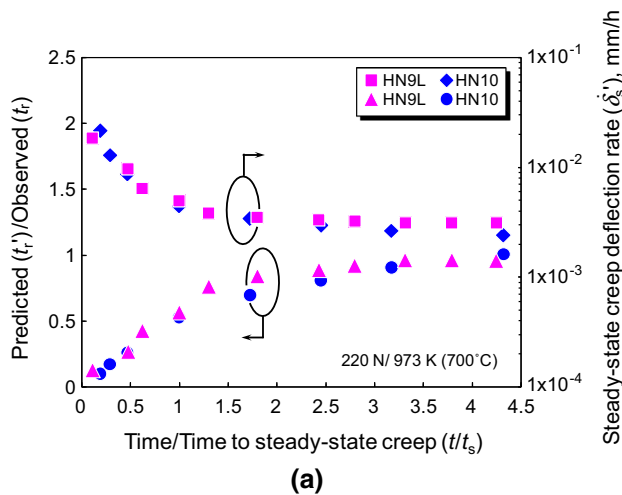
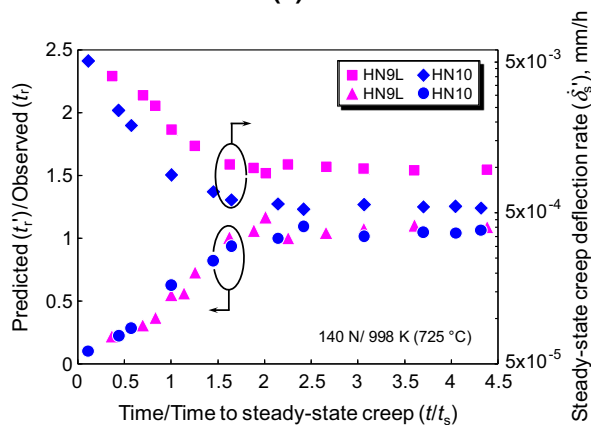


Fig. 9—Variation of steady-state deflection rate and minimum deflection rate with SP load at 973 K (700 °C).



(a)



(b)

Fig. 10—Accuracy of life prediction: (a) short creep time ($t_r \sim 200$ h) and (b) long creep time tests ($t_r \sim 1000$ h), in HN9L and HN10. Plots of variation of predicted steady-state deflection rate, $\dot{\delta}'_s$, and the ratio t'_r/t_r with time ratio t/t_s .

decreased with the increasing t/t_s until t/t_s was approximately 2.5, and then they showed almost no variation and attained constant values, exhibiting a steady-state. These constant values of $\dot{\delta}'_s$ were found to be the correct values of the steady-state deflection rates, $\dot{\delta}_s$, which were estimated from the complete creep curves. It can be seen that the ratio t'_r/t_r approached to 1 with the increasing t/t_s . The t'_r/t_r remained close to 1 when $t/t_s > 2.5$, which implied that in the steady-state creep region the predicted rupture lives were close to the observed rupture lives. Figure 11 illustrates the procedure of estimating steady-state deflection rate, $\dot{\delta}'_s$, during the creep test from the central deflection rate–time plot. This procedure was used in the above simulation for estimating the $\dot{\delta}'_s$. One should use the same procedure in an actual ongoing test for estimating $\dot{\delta}'_s$. In the above simulation, we started estimating $\dot{\delta}'_s$ after certain testing time t , when a rapidly decreasing deflection rate changed to a gradually decreasing deflection rate. In this test (HN10 at 1048 K (775 °C)/103N), we started estimating $\dot{\delta}'_s$ when the testing time was 71 hours. At 71 hours, the $\dot{\delta}'_s$ was

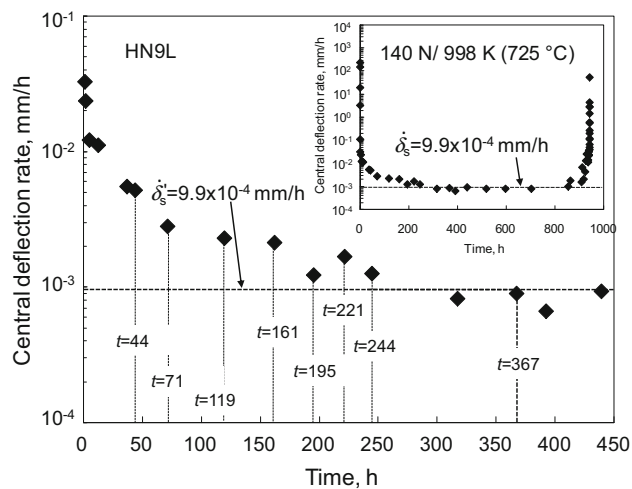


Fig. 11—Illustration of estimation of steady-state deflection rate, $\dot{\delta}'_s$, in SP creep test.

estimated as an average of deflection rates corresponding to 71 hours and its previous one (44 hours). With continuation of the test, the deflection rates gradually decreased, and the $\dot{\delta}'_s$ was estimated at each time as an average of the deflection rates at time t and its previous one. At some testing times, where the decrease in deflection rate was relatively small (71, 119, and 161 hours), more than two data points were considered for calculating the average $\dot{\delta}'_s$. In this case, the $\dot{\delta}'_s$ at 161 hours was estimated as an average of deflection rates corresponding to 71, 119, and 161 hours. Similarly, the $\dot{\delta}'_s$ at 244 hours was estimated as an average of the deflection rates corresponding to 195, 221, 244 hours. The above procedure was continued until the deflection rates showed almost no further decrease. In this test, the deflection rates were decreasing until the test time reached approximately 270 hours. After that, the central deflection rates remained constant, although some scatter was seen. The estimated $\dot{\delta}'_s$ at 367 hours (9.9×10^{-4} mm/h) was same as that $\dot{\delta}_s$ (9.9×10^{-4} mm/h) estimated after completion of the test by taking into account the whole steady-state creep stage (inset of Figure 11).

The accuracy of life prediction was assessed by comparing the predicted creep rupture life with the observed one at different testing times. Figure 12 shows the plot of predicted creep rupture life and the observed creep rupture life. The prediction was done at different testing times, *i.e.*, when t/t_s were 0.75, 1, 2, and 3, as shown in Figure 12(a), (b), (c), and (d), respectively. The graphs were plotted with an accuracy factor of 1.2. Here, the t_s was determined based on the steady-state deflection rate obtained from the least square method from the central deflection rate–time curves. The result shown in Figure 12(a), which was predicted when t/t_s was 0.75, corresponds to the testing time before the steady-state creep stage was attained. Therefore, a large scatter in the results was seen and the predicted life was much lower than the observed one. When t/t_s was 1

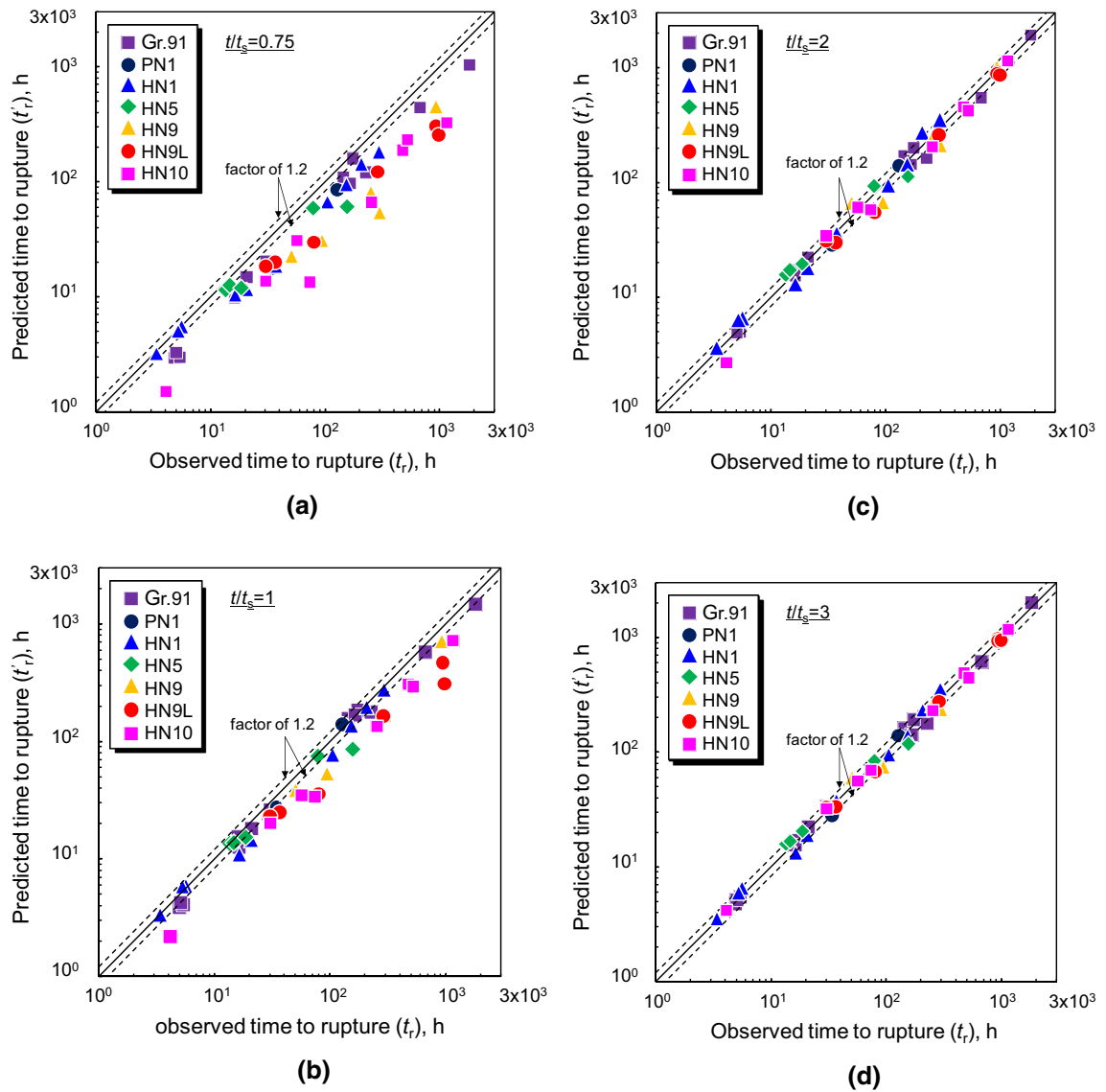


Fig. 12—Comparison of predicted times to rupture (t_r') with the observed ones (t_r): (a) $t/t_s=0.75$, (b) $t/t_s=1$, (c) $t/t_s=2$, and (d) $t/t_s=3$.

(Figure 12(b)), *i.e.*, when the steady-state creep stage was just begun, the accuracy of life prediction improved, although the predicted life was relatively lower than the observed one. With the increasing testing time, when t/t_s was 2 (Figure 12(c)), the prediction of creep rupture life could be achieved with a reasonably high accuracy. This indicated that it was possible to predict the rupture life accurately when the testing time was about two times the t_s . Further, the results shown in Figure 12(d) confirmed that the tests were still in the steady-state creep stage, and hence, the creep life could be predicted still accurately. Therefore, the creep rupture life could be predicted with a reasonably good accuracy within 30 to 40 pct of the creep rupture life. Hence, the rupture life can be predicted in the early stage of the creep test from the steady-state deflection rate without waiting until the minimum deflection rate is attained.

IV. CONCLUSIONS

The small punch (SP) creep deformation and rupture behaviors and their interrelationship were analyzed in different high-chromium ferritic heat-resistant steels. The central deflection rate–time behavior exhibited a steady-state creep stage. The time to onset of steady-state creep stage accounted for less than 30 pct of the creep rupture life. Both steady-state deflection rate and minimum deflection rate were found to be well correlated to the time to rupture and followed Monkman–Grant relation. These relationships were almost independent of the kind of steels studied, *i.e.*, whether the microstructure of the steel was martensite or ferrite, and hence could be represented by a master curve. The steady-state deflection rate–time to rupture relationship could be used for predicting SP creep rupture life and

the prediction was reasonably accurate within the factor of 1.2. The study revealed that this approach of rupture life prediction was advantageous over the prediction using the minimum deflection rate as the minimum deflection rate appeared in the latter half of the creep life. Therefore, SP creep rupture life can be predicted by conducting the creep test only until the steady-state creep stage without waiting for rupture of the specimen.

ACKNOWLEDGMENTS

This study was carried out as a part of the research activities of ALCA (Advanced Low Carbon Technology Research and Development Program). The financial support from JST (Japan Science and Technology Agency) is gratefully acknowledged. The authors sincerely thank the project Head and members for providing the uniaxial creep data for comparison.

REFERENCES

1. F. Monkman and N.J. Grant: *Am. Soc. Test. Mater. Proc.*, 1956, vol. 56, pp. 593–620.
2. J.D. Parker and J.D. James: in *Proceedings: 5th International Conference on Creep and Fracture of Engineering Materials and Structures*, Institute of Materials, 1993, pp. 651–60.
3. J. Ganesh Kumar, V. Ganesan, and K. Laha: *Metall. Mater. Tran. A.*, 2016, Vol. 47, Issue 9, pp. 4484–93.
4. S. Komazaki, T. Hashida, T. Shoji, and K. Suzuki: *J. Test. Eval.*, 2000, vol. 28, pp. 249–56.
5. N.C. Zan Htun, T.T. Nguyen, D. Won, M.H. Nguyen, and K.B. Yoon: *Mater. High Temp.*, 2017, vol. 34, Issue 1, pp. 33–40.
6. K. Milička and F. Dobeš: *Mater. Sci. Eng. A*, 2002, vol. 336, pp. 245–48.
7. B. Ule, R. Šturm, and V. Leskovšek: *Mater. Sci. Technol.*, 2003, vol. 19, pp. 1771–76.
8. R.C. Hurst, G.C. Stratford, and V. Bicego: in *Proceedings: ECCC Creep Conference*, 2005, pp. 349–58.
9. T. Nakata, S. Komazaki, Y. Kohno, and H. Tanigawa: *Exp. Mech.*, 2017, vol. 57 (3), pp. 487–94.
10. F. Dobeš and K. Milička: *Mater. Sci. Eng. A*, 2002, vol. 336, pp. 245–48.
11. S. Komazaki, T. Nakata, T. Sugimoto, and Y. Kohno: in *Advances in stainless steel*, B. Raj, ed., Universities Press, Boca Raton, 2009, pp. 135–45.
12. Y. Suzuki and Y. Nakatani: in *Proceedings: 3rd International Conference of SSTT*, K. Matocha, R. Hurst, W. Sun, eds., Austria, 2014, pp. 293–99.
13. M.D. Mathew, J. Ganesh Kumar, V. Ganesan and K. Laha: *Metall. Mater. Tran. A*, 2014, vol. 45, pp. 731–37.
14. J. Ganesh Kumar and K. Laha: *Mater. Sci. Eng. A*, 2015, vol. 641, pp. 315–22.
15. S. Komazaki, T. Tokunaga, and Y. Kawaji: in *Proceedings: 3rd International Conference of SSTT*, K. Matocha, R. Hurst, W. Sun, eds., Austria, 2014, pp. 312–18.
16. Naveena and S. Komazaki: *Mater. Sci. Eng. A*, 2016, vol. 676, pp. 100–08.